

Clustering effects on the heating performance of magnetic nanoparticles

Author: Oriol Peraire Tubau

*Facultat de Física, Universitat de Barcelona, Diagonal 645, 08028 Barcelona, Spain.**

Advisor: Òscar Iglesias

Abstract: Magnetic nanoparticle (NP) hyperthermia has risen high expectations as an alternative therapy for treating cancer. However, in order to compete with existing therapies, the heat delivered under application of an alternating needs to be maximized keeping the NP concentration at a minimum. For this purpose, an appropriate choice of external parameters and material characteristics is required. In the present study, we will use Monte Carlo simulations of dipolar interacting assemblies of NP to study how the size of the NP, their degree of clustering and concentration, as well as the applied magnetic field can be tuned in order to get the maximum delivered heat power. In particular, we will show that particular spatial distributions of the NP minimize the detrimental influence of the unavoidable interparticle interactions.

I. INTRODUCTION

Magnetic particle hyperthermia is a proposed therapy based on killing cancerous cells by applying heat to them through magnetic nanoparticles (NPs) under an alternating magnetic field (AMF). The main feature of the therapy is the usage of nanoparticles. Their small size is a great advantage, making the therapy really local and not invasive at all, compared to chemical-radiative based therapies. With this characteristic it is possible to reduce the heat exposure of healthy tissues and focus it more to the cancerous cells¹. Moreover, this therapy has great synergy with other actual therapies, the interaction of heating the cells and the wide range of drugs used in chemotherapy or with the radiation, makes the desirable cells more susceptible to their effects. Therefore magnetic hyperthermia is not only compatible with other therapies, furthermore it increases their effectiveness². On the other hand, nowadays the magnetic fluid concentration administrated to the patient is quite high¹ and the magnetic available NP's for *in vivo* applications are considerably limited due to biocompatibility and legal reasons³. In our study, we will focus on the optimization of the NPs' thermal capabilities. In order to do so, we will simulate different systems formed by magnetic NPs modifying some parameters of the system at a time and observing which one gives more significant results. We will first introduce the theory on which we have based our study on and the relevant parameters. We will then explain the simulation method followed, discussing its pros and cons and some technicalities. Finally, we will show the obtained results, discussing the NP size effects, studying the effect of NP concentration and comparing different NPs cluster distributions, and finally we will show the effect of having minor hysteresis loops.

II. BASIC THEORETICAL MODEL

Our magnetic system is made of an assembly of interacting magnetic NP randomly distributed in space in

different ways. We will work with a variation of the Stoner-Wohlfarth model², in which we will include the dipolar interaction between NPs. The Stoner-Wohlfarth (SW) model is a micromagnetic model that considers each NP as a macrospin, disregarding its internal structure. Therefore, the relevant energies are associated to the magnetocrystalline anisotropy (which we will consider for simplicity uniaxial) and the Zeeman energy. The associated energy density can be written

$$\frac{E_T}{V} = K_u \sin^2 \theta - \mu_0 M_s H(t) \cos(\alpha - \theta), \quad (1)$$

where θ is the angle between the magnetization and the easy-axis, α is the angle between the applied field and the easy-axis, K_u is the uniaxial anisotropy constant, μ_0 is the vacuum permeability and M_s the spontaneous magnetization.

When the applied field is zero, we find the two minimum energy states along the easy-axis direction, separated by an energy barrier $\varepsilon_B = K_u V$. When an external field is applied, the symmetry of these two states is broken, one state has less energy than the other, lowering the ε_B between them. ε_B decreases also when reducing the NP size. So that, below a critical size, the barrier can be overcome by thermal fluctuations during the measurement time, reaching the so-called superparamagnetic (SP) limit, below which the area of the hysteresis loop drops to 0.

The dipolar energy between two interacting magnetic moments m_i and m_j is given by classical magnetostatics as²

$$E_d(\vec{m}_i, \vec{m}_j, \vec{r}_{ij}) = \frac{\mu_0}{4\pi} \left[\frac{\vec{m}_i \cdot \vec{m}_j}{r_{ij}^3} - 3 \frac{(\vec{m}_i \cdot \vec{r}_{ij})(\vec{m}_j \cdot \vec{r}_{ij})}{r_{ij}^5} \right], \quad (2)$$

where r_{ij} is the distance between them. Thus, to compute the total dipolar energy for an assembly of particles, a double sum over the N is required, which can be computationally very demanding in a Monte Carlo (MC) simulation if it is done by brute force. In the next section, we will introduce some computational techniques to improve the performance of the required calculations.

As we mentioned before, the objective of our study is to increase the power dissipated by our magnetic NPs without causing serious side effects. This magnitude, called specific absorption rate (*SAR*) is given by⁴

$$SAR = \frac{Af}{\rho}, \quad (3)$$

measured in $\frac{W}{g}$, where A is the area of the HL (i.e. $A = \int_{-H_{\max}}^{+H_{\max}} \mu_0 M(H) dH$), f the frequency of the AMF and ρ the density of the magnetic material.

In principle, within the scope of our model, we have different parameters that can be tuned in order to optimize *SAR*, but in practice, this cannot be done at will since several biological and methodological limitations impose some restrictions. First, there is a limit in the magnitude and frequency of applied magnetic fields to living tissues, known as Brezovich criterion $H \cdot f = 4.5 \times 10^8 \text{ A}/(\text{m} \cdot \text{s})^1$. There are also biocompatibility and toxicity issues to be respected, that limit the choice of materials for the magnetic NPs. The material parameters chosen for our simulations correspond to Fe oxides, typically in the form of magnetite or maghemite. These materials are among the few with notable magnetic properties approved for biomedical applications by the European Medicine Agency and the Food and Drug Administration of USA. Also, their metabolic route is well defined. Even so, NPs with other compositions have been proposed for this application, such as Fe oxides doped with other metals as Co^{3+} , that should be properly covered by protecting shells to prevent toxicity.

The geometries and spatial distributions of the NPs are limited by our technology and the control of them when they are inserted in the tissue and finally reach the cancerous cells. However, some pseudo-realistic geometries will be studied in the following sections together with the concentration, particle radius and maximum magnetic field applied. Finally, as we will describe in the next section, since a direct mapping between MC steps and real time cannot be established consistently, we will not vary the frequency of the external field.

III. COMPUTATIONAL METHOD

The simulations are done based on the typical MC Metropolis method applied to classical Heisenberg spins. Our goal is to study HLs, which occur out of equilibrium, since their area is directly proportional to the *SAR*. In the pseudodynamic-MC method⁵ used here the HL protocol is mimicked by slightly changing the field applied for a certain number of MCS. In our case, we chose a total of 80000 MCS and 800 MCS for each applied field⁶. The MCS can be thought as the time we wait between two measures in an experiment. So, the simulated HL will also depend slightly on the number of MCS we use to average the magnetization at a given field. Therefore, in principle, we could tune up the simulations to change

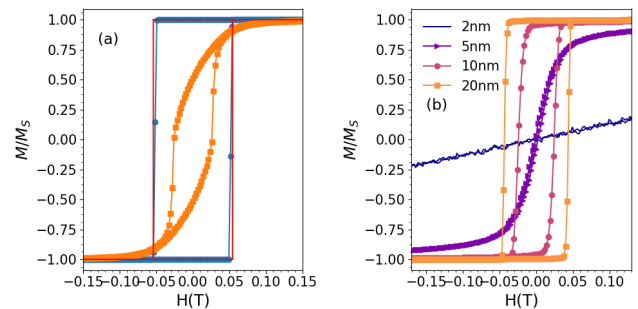


FIG. 1: (a) Comparison between the results predicted by the Stoner-Wohlfarth model (red) and our simulation for the HL of a non-interacting assembly of magnetite NP with aligned easy-axes (blue) or pointing at random directions (orange) at $T = 5K$. (b) HL for a non-interacting assembly of magnetite NP with aligned easy-axes of different NP radii as indicated in the legend at $T = 300K$.

the frequency of the AMF. The problem is that we do not have a mapping between MCS of our code and time.

At each MCS a random NP with magnetic moment pointing along \hat{S}_{old} is selected and a new state \hat{S}_{new} accepted or rejected following the Metropolis algorithm, which takes into account the energy change between them. The new state is chosen at random but inside a cone of a given aperture $a = 0.3$ with respect to the old state. In this way, we ensure a control over the dynamics of the system and correct sampling of the energy barriers in between states.

In order to treat the dipolar term in an efficient and simple way we write Eq. 2 as:

$$E_d(\vec{m}_i, \vec{m}_j, \vec{r}_{ij}) = \hat{S}_i W_{ij}(\vec{r}_{ij}) \hat{S}_j \quad (4)$$

Where W_{ij} have to be computed only at the beginning of the simulation, after positioning each particle:

$$W_{ij}^{\alpha\beta} = \frac{\delta_{ij}}{r_{ij}^3} - \frac{3\delta_{\alpha\gamma}\delta_{\beta\eta}r_{ij}^\gamma r_{ij}^\eta}{r_{ij}^5}. \quad (5)$$

As we can see W_{ij} is a symmetric tensor, so we will only need to compute six matrices referring to each combination of the components.

In order to check the code and algorithms, preliminary simulations were done for non-interacting assemblies ($\Phi \rightarrow 0$). The simulated HL compare satisfactorily with those obtained analytically using the SW model as can be seen in Fig. 1 (a), where the small departures from the model are due to temperature effects. We also observe the reduction of the HL area in the case where the easy-axis are pointing in random directions compared to the case where all the particles easy-axes are aligned to the external magnetic field. The simulations have been done using the computer Pirineus II of CSUC.

IV. RESULTS

Several simulations have been done observing the effects of changing different parameters on the HL, we have focused in size, concentration, saturation magnetic field and spatial distribution. As we explained in the Sec.II, we have chosen magnetic parameters corresponding to magnetite, $K = 13000 \text{ J/m}^3$ and $M_S = 480000 \text{ A/m}$. Temperature will be fixed at $T = 300 \text{ K}$ in all simulations (unless otherwise stated) and a cut-off (a minimum distance imposed between NPs) of $0.25R$ will be considered also. The number of particles is kept constant at $N = 1000$. In order to achieve a random distribution in space with volume concentration Φ , we vary the size of the simulation volume according to $R_{sim} = (N/\Phi)^{1/3}R$. We will study NP assemblies with anisotropy easy-axes either aligned along the field direction or pointing at random. Results for non-interacting assemblies will be shown only in the first subsection in order to compared them with the interacting case.

First, we will discuss the size effects of NPs in a random spherical distribution and finding the SP limit. Next, we will discuss the effects of spatial distribution of the NPs in different distributions, and the variation of the HL area with the concentration. In spite of this, SAR can be increased also in interacting assemblies using bigger particles or, as will be shown in Sec. IV B, increasing the cut-off distance. Finally, we will study minor loops and their implication in the HL area.

A. Size effects

The first aspect studied is the impact that the NP size has in the HL. We expect to find a critical size below which the SP state is achieved at $T = 300 \text{ K}$ and that this will be different in non-interacting and interacting NPs. In Fig. 1 (b), we see that when reducing the NP radius in a non-interacting assembly ($\Phi \rightarrow 0$) with aligned easy-axes, the HL area decreases. For $R = 5 \text{ nm}$ the area enclosed by the HL is already near zero, resembling the SP case. For $R = 2 \text{ nm}$ thermal noise dominates over the magnetic energies.

By looking at the dependence of the HL area on radius presented in Fig 2 (a), we have a better insight of this effect, observing a great decay of the area for $R < 12.5 \text{ nm}$, reaching zero values for $R = 5 \text{ nm}$ in the case of non-interacting NPs and $R = 6 \text{ nm}$ for interacting ones with $\Phi = 0.1$. This effect is explained by the reduction of the energy barrier which is proportional to the volume of the particle and it is the responsible of maintaining the ferromagnetic state. Thermal excitations would be sufficient for the particle to cross the energy barrier, resulting in a null magnetic remanence. In order to get sufficient SAR (large HL area), we should focus in NPs with radius between 12.5 nm to 20 nm , where the single domain approximation still holds for Fe oxides.

In the same figure, we can also appreciate that adding

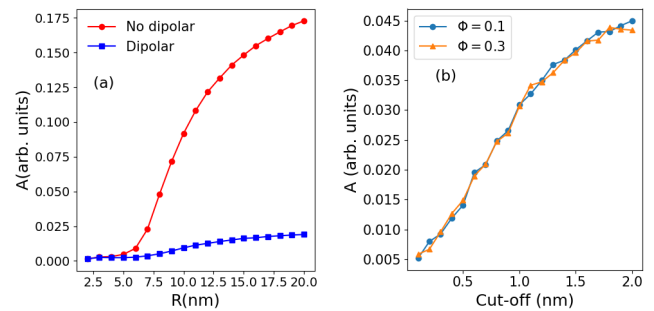


FIG. 2: Panel (a) HL area for NP in random positions inside a sphere with the easy-axis aligned to the external magnetic field as a function of the NP radii. In panel (b), we represent the HL area as a function of the cut-off distance for a random distribution of aggregates of 3 inside a sphere for different concentrations, with their easy-axes pointing at random positions.

dipolar interactions between the NPs, drastically reduces the HL area, demonstrating the non-desirable effects of clustering and aggregation on SAR also observed experimentally. In what follows, we will consider only NP with a radius $R = 15 \text{ nm}$.

B. Concentration and geometry effects

The alteration of the NPs magnetic properties due to the interaction with the physiological media has been observed in several experiments, obtaining lower heating performance of the NPs than expected, caused by the aggregation and clustering effects. However, M. P. Morales et al.⁷ have obtained promising results encapsulating the NP inside liposomes in order to get different controlled spatial distributions depending on the coating used. The group of T. Pellegrino⁸ have also been able to compare results of NP samples with clusters of different sizes. In order to model the spatial distribution of the NP in real assemblies, three simplified models have been considered in the simulations: (1) randomly distributed NP inside a spherical volume, (2) Randomly distributed NP on the surface of a spherical shell with thickness equal to the NP diameter, (3) Clusters of 3 NP randomly distributed in a spherical volume.

In Fig. 3(a), the HLs for the three models with the same concentration $\Phi = 0.1$ are compared. As a consequence of the interactions, the HL high closure fields and both the coercive field and remanent magnetization decrease with respect to the non-interacting case, resulting in a decrease of the HL general in the 3 cases. These result is in agreement with a similar simulation study using other methods by U. Nowak et al.⁹. However, we observe that (even if we keep the same volume concentration) these quantities clearly depend on how the NP are distributed in space, causing appreciable changes in the area of the HL.

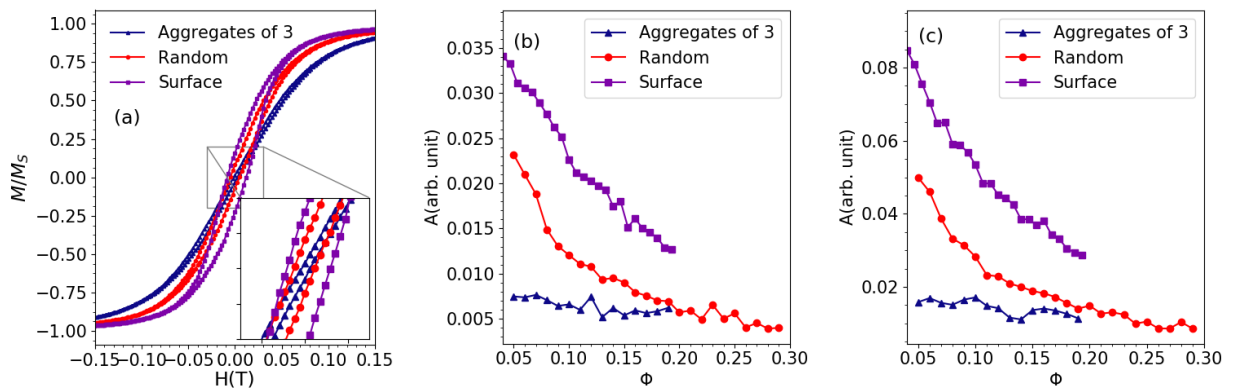


FIG. 3: (a) HL for an assembly of NP randomly distributed inside a sphere, at the surface of a sphere, and forming clusters of three inside a sphere with $\Phi = 0.1$ and random distribution of easy-axes. (b) Variation of the HL area of assemblies with aligned easy-axes with concentration Φ for the three previous cases. (c) The same as (b) but for assemblies with random distribution of easy-axes.

These can be better appreciated in Fig. 3 (b) and (c), where this quantity is represented as a function of Φ for aligned and randomly oriented assemblies. First, we see that for models 1 and 2, the HL area decreases rapidly with Φ due to the strong interparticle separation dependence ($1/r^3$) of the dipolar interaction, that decreases with increasing concentration. However, the area varies much smoothly with Φ for model 3, indicating that, in that case, the dipolar interaction between the NP in the individual clusters dominates over the inter-cluster interactions, independently of the concentration. Most remarkable is the fact that the HL area is much increased in model 2, which has NP distributed on a surface, with respect to the two others. This is probably since the NP have further separated neighbours across the inner part of the surface on which they are distributed as compared to model 1.

However, 2 (b) shows that increasing the cut-off distance between the clusters for two different concentrations for a distribution of 3-aggregates implies an increase of the area, although increasing the concentration does not significantly decrease it. The cut-off is imposing a minimum distance between clusters, so the dipole interaction is reduced implying an increase of the area much more efficient than if we just reduce the concentration. This could be achieved experimentally by increasing the minimum separation between the NP with use of surfactants or covering of the NP with functional molecules.

C. Minor hysteresis loops

In this section, we analyse the effect that the maximum AMF applied (H_S) during the HL has on the SAR . As has already been mentioned in Sec. II, the magnitude and frequency of the AMF that can be used in a magnetic hyperthermia therapy is limited by physiological criteria. Therefore, if higher frequencies are applied to increase

the area of the HL (see Eq. 3), H_S has to be reduced below the saturation field, with the consequent decrease of the HL area due to minor loop effects. This can be clearly observed in the simulation results of Fig. 4 (a), where for $H_S < 0.08$ T corresponding to the closure field of the HL, minor loops appear. The calculated areas for different H_S follow a similar decreasing trend with Φ for all the studied H_S as can be seen in Fig. 4 (b), indicating that lower concentrations should be used if H_S diminishes if SAR is to be maximized.

It is customary in the literature to use linear response theory (LRT)¹⁻³, valid for low fields and non-interacting assemblies, when analysing SAR dependencies on the different parameters. According to LRT, SAR should increase as H_S^2 , although in many experimental reports this law is not observed, and many contradictory results have been published for in different field regimes. Our simulations results shown in Fig. 4 (c) are valid beyond the approximations used in LRT and should be regarded as an extension of this model when interactions are included and valid up to saturating fields. As it can be clearly seen, the HL area shows a progressive non-monotonous variation with H_S , with a region of steeper increase that extends to higher values of H_S with increasing Φ and a region with more moderate increase as H_S approaches the closure fields.

V. CONCLUSIONS

Several systems of Fe oxide NP assemblies under an external magnetic field have been studied numerically in order to observe the effect of modifying NP's size, spatial distribution, concentration and H_S on the HL areas, which are directly related to the SAR . First, we have found a limited particle size range ($R = 5 - 20$ nm) for the efficiency of hyperthermia treatment. However, we have found that sizes $R \gtrsim 12.5$ nm are necessary in order

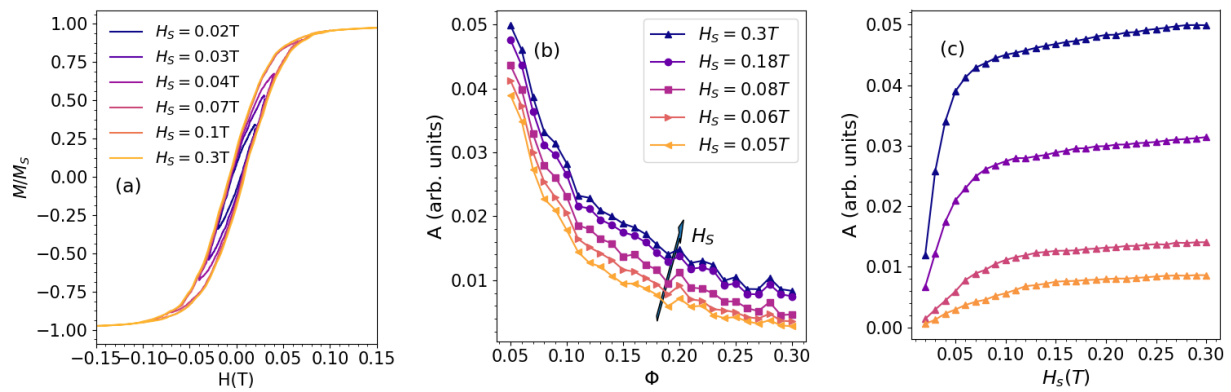


FIG. 4: Panel (a) shows HLs for an assembly of NP distributed in a spherical volume, $\Phi = 0.1$ and aligned easy-axes for different maximum applied fields (H_S). Panel(b) presents the HL area dependence on the concentration Φ for different H_S . Panel (c) displays the dependence of the HL area on H_S for increasing concentrations 0.06, 0.1, 0.2 and 0.3 from upper to lower curves. In (b) and (c) the easy-axes directions are random

to maximize the SAR .

The obtained results show that the existence of dipolar interactions in concentrated samples can drastically reduce the HL area and, therefore, limit the efficacy of hyperthermia therapies, at least in NP assemblies with some degree of clustering and randomness in spatial distribution, in agreement with studies⁹ based on other simulation methods. This is the main drawback of increasing the dose of delivered NP, that causes an increase in concentration. However, the most remarkable result with may have a direct impact on current experimental studies in tumorous cells is related to geometric effects. We have shown that placing the NP at the surface of a given volume is considerably more efficient regarding SAR than if they are inside it. This finding shows that, as far as the magnetic dissipation contribution is concerned, attaching the NP on the cellular membrane (which can be easier to achieve) might be advantageous and that there might be no need to find a way to internalize the NP inside the cell to induce their death. In contrast, we have shown that the

clustering of the NP, even in small units, produces much more noticeable reduction of the HL areas. The results on this class of agglomerates deserve further theoretical study, since some experimental works (see for example Ref. 8) have shown indications that highly anisotropic clusters can improve the heating capabilities.

Finally, we have shown that HL areas increase with the increase of the magnitude of the maximum applied field to values higher than the closure field, which in contrast should be low enough so that the physiological limits are respected. Our calculations extend the limit of validity of the LRT to the high field range and by inclusion of interactions, which is not possible in analytical expressions.

Acknowledgments

I would like to give my special thanks to Dr. Òscar Iglesias for investing an insane amount of hours in this work and CSUC computational resources.

* Electronic address: operaire97@gmail.com

- ¹ D. Ortega and Q. A. Pankhurst, *Magnetic hyperthermia in Nanoscience: Volume 1: Nanostructures through Chemistry*, (Royal Society of Chemistry: Cambridge 2013, P. O'Brien ed.) pp 60-88.
- ² K. M. Krishnan, *Fundamental and applications of magnetic materials*, (Oxford Unity Press: 2016, 1st. ed.).
- ³ C. Blanco-Andujar, F. J. Teran, D. Ortega, *Iron Oxide Nanoparticles for Biomedical Applications: Synthesis, Functionalization and Application*, (Metal Oxides series 2018, 1st. ed.) pp 197-245.
- ⁴ J. Carrey, B. Mehdaoui and M. Respaud, *Simple models for dynamic hysteresis loop calculations of magnetic single-domain nanoparticles: Application to hyperthermia optimization*, *J. Appl. Phys.* **109**, 083921 (2011).
- ⁵ A. Yamaguchi et al., *Applications of Monte Carlo Method*

in Science and Engineering, (InTech 2011, Prof. Shaul Mordechai Edition) pp 513-561

- ⁶ Yu. L. Raikher et al., *Time quantification for Monte Carlo modeling of superparamagnetic relaxation* *Physical Review B* **86**, 104423 (2012)
- ⁷ M. P. Morales et al., *Magnetic properties of nanoparticles as a function of their spatial distribution on liposomes and cells* *Phys. Chem. Chem. Phys.*, 101039 (2018)
- ⁸ D. Niculaes et al., *Asymmetric Assembling of Iron Oxide Nanocubes for Improving Magnetic Hyperthermia Performance* *ACS Nano* **11**, 12121-12133 (2017)
- ⁹ U. Nowak and C. Haase, *Role of dipole-dipole interactions for hyperthermia heating of magnetic nanoparticle ensembles* *Physical Review B* **85**(4), 101103 (2012)